Inductively Heated Incompressible Flow of Electrically Conductive Liquid in Pipe

I. Dolezel[1,2], L. Dubcova[2], P. Karban[3], J. Cerveny[2], and P. Solin[2,4]

[1]Faculty of Electrical Engineering, Czech Technical University, 166 27 Praha 6, Czech Republic
[2]Department of Electrophysics, Academy of Sciences of the Czech Republic, Institute of Thermomechanics, v.v.i. 182 00 Praha 8, Czech Republic
[3]Faculty of Electrical Engineering, University of West Bohemia, 306 14 Plzen, Czech Republic
[4]Department of Mathematics and Statistics, University of Nevada, Reno, NV 89557-0208 USA

A novel computer model of inductively heated incompressible flow of electrically conductive liquid in a pipe is presented. The numerical solution of this multiply coupled problem is realized by a higher-order finite element method using the code Hermes2D developed and written by the authors. The algorithm contains a number of original features such as hanging nodes of any order or in time adaptively changing mutually independent meshes for the computation of particular time-dependent field quantities. The methodology is illustrated by a typical example whose results are discussed.

***Index Terms*—Electromagnetic field, flow field, higher-order finite element method, incompressible flow, induction heating, numerical analysis, temperature field.**

I. Introduction

NUMEROUS industrial technologies working with electrically conductive liquids (e.g., molten metals, acids or solutions of salts) are based on the force and thermal effects of electromagnetic field. We can mention pumping, dosing, stirring, heating, and other similar processes.

The computer modeling of such processes is still a challenge. These tasks usually represent multiply coupled nonstationary and often nonlinear problems, characterized by interaction of several physical fields. The flow itself can be accompanied by turbulences and local phenomena that are difficult to map. Even when a considerable attention is paid to the topic (the books and papers in the domain abound, see, e.g., [1], [2]), a lot of tasks were solved only partially or still remain unresolved.

The paper deals with the problem of heating a conductive liquid flowing at a slow velocity in a ceramic pipe. Its numerical solution is carried out (unlike former classical finite elements and finite volumes-based algorithms) by our own code Hermes [3] based on the higher-order finite element method (*hp*-FEM).

II. Formulation of the Problem

Consider the arrangement depicted in Fig. 1. The figure shows a ceramic pipe with electrically conductive liquid that flows from the left to the right and is both heated up by a time-variable magnetic field generated by a harmonic current carrying inductor and accelerated by the corresponding Lorentz forces. The arrangement of the system is assumed axisymmetric.

The task is to map the time evolution of all physical fields in the system, namely magnetic field, temperature field, field of the radial and axial components of the velocity of flow, and field of pressure. The physical parameters of the liquid, pipe, and inductor are supposed to be known, as well as the relevant initial and boundary conditions, and also the parameters of the field current (its amplitude I and frequency f).

Manuscript received December 22, 2009; accepted February 17, 2010. Current version published July 21, 2010. Corresponding author: I. Dolezel (e-mail: dolezel@it.cas.cz).

Color versions of one or more of the figures in this paper are available online at http://ieeexplore.ieee.org.

Digital Object Identifier 10.1109/TMAG.2010.2044488

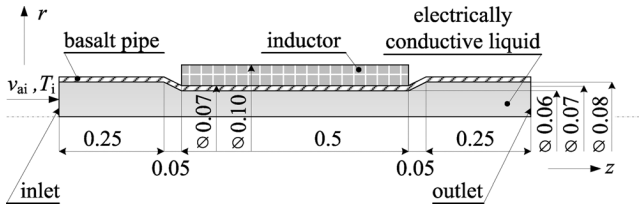

Fig. 1. Investigated arrangement (all dimensions are in m).

III. Continuous Mathematical Model

The mathematical model of the problem is given by three partial differential equations describing the distribution of the magnetic field, the temperature field and the field of flow. These equations are mutually linked by the presence of the velocity of liquid in each of them.

A. Magnetic Field

The distribution of the magnetic field may be best expressed in terms of the magnetic vector potential $\boldsymbol{A} = \boldsymbol{A}(r, z)$. Since the system contains no nonlinear parts, we can use its phasor $\underline{\boldsymbol{A}}$ that is governed by the equation

$$(\operatorname{curl} \underline{\boldsymbol{A}}) + \mathrm{j} \cdot \omega\gamma\mu\, \underline{\boldsymbol{A}} - \gamma\mu \boldsymbol{v} \times \operatorname{curl} \underline{\boldsymbol{A}} = \mu\, \underline{\boldsymbol{J}}_{\mathrm{ext}} \qquad (1)$$

where μ denotes the magnetic permeability ($\mu = \mu_0$), γ is the electric conductivity, ω is the angular frequency, $\boldsymbol{v}$ is the vector of the velocity of flow, and $\underline{\boldsymbol{J}}_{\mathrm{ext}}$ stands for the phasor of the external harmonic current density in the inductor.

In the axisymmetric arrangement each of the phasors $\underline{\boldsymbol{A}}$ and $\underline{\boldsymbol{J}}_{\mathrm{ext}}$ has only one nonzero component in the tangential direction α, while the vector of velocity $\boldsymbol{v}$ has two nonzero components v_r, v_z in the directions of r and z. For this case (1) can be written as follows:

$$\frac{\partial^2 \underline{A}_\alpha}{\partial r^2} + \frac{1}{r}\frac{\partial \underline{A}_\alpha}{\partial r} - \frac{\underline{A}_\alpha}{r^2} + \frac{\partial^2 \underline{A}_\alpha}{\partial z^2} - \mathrm{j} \cdot \omega\gamma\mu \underline{A}_\alpha - \mu\gamma v_r \left(\frac{\partial \underline{A}_\alpha}{\partial r} + \frac{\underline{A}_\alpha}{r} \right) - \mu\gamma v_z \frac{\partial \underline{A}_\alpha}{\partial z} = -\mu \underline{J}_{\mathrm{ext},\alpha}. \qquad (2)$$

The axis z of the arrangement and sufficiently distant artificial boundary are characterized by the Dirichlet boundary condition $\underline{A}_\alpha = 0$.

The harmonic magnetic field (the phasor of its magnetic flux density $\underline{\boldsymbol{B}}(r,z) = \operatorname{curl} \underline{\boldsymbol{A}}(r,z)$ has two components $\underline{B}_r(r,z)$ and $\underline{B}_z(r,z)$) generates in electrically conductive liquid eddy currents consisting of two components due to transformation and movement. The phasor of the local density $\underline{\boldsymbol{J}}$ due to these eddy currents is given by the expression

$$\underline{\boldsymbol{J}} = -\mathrm{j}\cdot\omega\gamma\,\underline{\boldsymbol{A}} + \gamma v \times \operatorname{curl}\underline{\boldsymbol{A}} = -\mathrm{j}\cdot\omega\gamma\underline{\boldsymbol{A}} + \gamma\boldsymbol{v}\times\underline{\boldsymbol{B}} \quad (3)$$

which, in the considered axisymmetric arrangement, may be rewritten into the form

$$\underline{J}_\alpha = -\mathrm{j}\cdot\omega\gamma\underline{A}_\alpha + \gamma v_r\left(\frac{\partial\underline{A}_\alpha}{\partial r} + \frac{\underline{A}_\alpha}{r}\right) + \gamma v_z\frac{\partial\underline{A}_\alpha}{\partial z}. \quad (4)$$

These induced currents produce both heating of the liquid and also forces acting on its particles. Heating is caused by the Joule losses whose local average (in one period) values p_{Ja} follow from the formula

$$p_{\mathrm{Ja}} = \frac{|\underline{J}_\alpha|^2}{\gamma} \quad (5)$$

while the local (volumetric) Lorentz forces $\boldsymbol{f}_{\mathrm{L}}$ are generally given as

$$\boldsymbol{f}_{\mathrm{L}} = \boldsymbol{J}\times\boldsymbol{B} = \boldsymbol{J}\times\operatorname{curl}\boldsymbol{A}. \quad (6)$$

In the axisymmetric case these forces have just two nonzero components—$f_{\mathrm{L}r}$ in the r -direction and $f_{\mathrm{L}z}$ in the z-direction. Both of them are functions of the velocity $\boldsymbol{v}$. Their average values $f_{\mathrm{La}r}$ and $f_{\mathrm{La}z}$ in one period follow from the formulas

$$\begin{aligned} f_{\mathrm{La}r} &= \frac{1}{2}|\underline{J}_\alpha||\underline{B}_z|\cos(\arg(\underline{J}_\alpha) - \arg(\underline{B}_z)) \\ f_{\mathrm{La}z} &= -\frac{1}{2}|\underline{J}_\alpha||\underline{B}_r|\cos(\arg(\underline{J}_\alpha) - \arg(\underline{B}_r)). \end{aligned} \quad (7)$$

B. Temperature Field

The nonstationary heat transfer equation in the liquid continuum reads

$$\operatorname{div}(\lambda\cdot\operatorname{grad}T) = \rho c\cdot\left(\frac{\partial T}{\partial t} + v\cdot\operatorname{grad}T\right) - p_{\mathrm{Ja}} \quad (8)$$

where λ is the thermal conductivity, ρ is the specific mass, c denotes the specific heat at constant pressure, and v stands for the velocity. Finally, the symbol p_{Ja} denotes the time average internal sources of heat (the specific Joule losses) determined by formula (5). In the axisymmetric arrangement temperature T is only a function of space variables r, z and time t, so that (8) may easily be transformed into the form

$$\begin{aligned} &\frac{\partial}{\partial r}\left(\lambda\frac{\partial T}{\partial r}\right) + \frac{\lambda}{r}\left(\frac{\partial T}{\partial r}\right) + \frac{\partial}{\partial z}\left(\lambda\frac{\partial T}{\partial z}\right) \\ &\qquad = \rho c\cdot\left(\frac{\partial T}{\partial t} + v_r\frac{\partial T}{\partial r} + v_z\frac{\partial T}{\partial z}\right) - p_{\mathrm{Ja}}. \end{aligned} \quad (9)$$

The temperature field is calculated only in the liquid and in the pipe, where, however, the term $\boldsymbol{v}\cdot\operatorname{grad}T$ vanishes. The boundary condition along the external surface of the pipe only respects the convection (basalt is a poor thermal conductor, thus the temperature of this surface is low and radiation from it can be neglected). The temperature of the liquid at the inlet of the pipe is supposed to be known. The axis of symmetry (z-axis) is characterized by the zero Neumann boundary condition.

C. Field of Flow

The field of incompressible flow will be supposed Newtonian, obeying the Navier-Stokes equation

$$\rho\cdot\left[\frac{\partial\boldsymbol{v}}{\partial t} + (\boldsymbol{v}\cdot\operatorname{grad})\boldsymbol{v}\right] = -\operatorname{grad}p + \eta\cdot\Delta\boldsymbol{v} + \boldsymbol{f}_{\mathrm{v}} \quad (10)$$

together with the equation of continuity

$$\operatorname{div}\boldsymbol{v} = 0. \quad (11)$$

Here, p is the pressure, η is the dynamic viscosity, and $\boldsymbol{f}_{\mathrm{v}}$ stands for the sum of internal volumetric driving forces. This sum includes the Lorentz force $\boldsymbol{f}_{\mathrm{L}}$ (6), specific weight of melt $\boldsymbol{f}_{\mathrm{g}}$, and specific force $\boldsymbol{f}_{\mathrm{b}}$ acting on the particles of melt due to nonhomogeneous distribution of temperature in it. For the practical computations, the last two components will be ignored (with a negligible error) in order to preserve the axial symmetry of the flow.

Now, after rewriting (10) and (11) in the axisymmetric arrangement we obtain

$$\begin{aligned} &\rho\cdot\left[\frac{\partial v_r}{\partial t} + v_r\frac{\partial v_r}{\partial r} + v_z\frac{\partial v_r}{\partial z}\right] \\ &\quad = -\frac{\partial p}{\partial r} + \eta \\ &\qquad\cdot\left(\frac{\partial^2 v_r}{\partial r^2} + \frac{1}{r}\frac{\partial v_r}{\partial r} - \frac{v_r}{r^2} + \frac{\partial^2 v_r}{\partial z^2}\right) + f_{\mathrm{La}r} \end{aligned} \quad (12)$$

$$\begin{aligned} &\rho\cdot\left[\frac{\partial v_z}{\partial t} + v_r\frac{\partial v_z}{\partial r} + v_z\frac{\partial v_z}{\partial z}\right] \\ &\quad = -\frac{\partial p}{\partial z} + \eta \\ &\qquad\cdot\left(\frac{\partial^2 v_z}{\partial r^2} + \frac{1}{r}\frac{\partial v_z}{\partial r} + \frac{\partial^2 v_z}{\partial z^2}\right) + f_{\mathrm{La}z} \end{aligned} \quad (13)$$

$$\frac{\partial v_r}{\partial r} + \frac{v_r}{r} + \frac{\partial v_z}{\partial z} = 0. \quad (14)$$

The boundary conditions are of the classical type—the velocity along the internal wall of the pipe vanishes, due to the axial symmetry its radial component vanishes along the z-axis and the derivative of its axial component with respect to the radius r also vanishes here. The profile of the velocity v_{i} at the inlet (see Fig. 1) follows from knowledge of the initial state of the system.

IV. Numerical Solution

The numerical solution of the problem is realized by an adaptive *hp*-FEM. It is a modern version of the finite element method combining finite elements of variable size (h) and polynomial degree (p) in order to obtain fast exponential convergence [4]. For the discretization of incompressible fluid flow we use well known Taylor-Hood Q2/Q1 elements (biquadratic elements for velocities and bilinear elements for pressure) that satisfy the inf-sup condition. Since the Reynolds numbers in our problems are large, an approximate solution can contain nonphysical spurious oscillations. In order to avoid them, we apply the stabilization by the streamline-diffusion method combined with the pressure stabilization [5].

TABLE I
PHYSICAL PARAMETERS OF MOLTEN SODIUM

quantity	unit	value
specific mass ρ	kg m^{-3}	927
temperature of melting T_m	°C	97.72
electrical conductivity γ	S m^{-1}	2.0964×10^6
thermal conductivity λ	W m^{-1} K^{-1}	142
thermal capacity c	J kg^{-1} K^{-1}	1230
dynamic viscosity η	Pa s	for 98 °C 0.000688 for 127 °C 0.000599 for 227 °C 0.000415

TABLE II
PHYSICAL PARAMETERS OF BASALT

quantity	unit	value
specific mass ρ	kg m^{-3}	2900
electrical conductivity γ	S m^{-1}	0
thermal conductivity λ	W m^{-1} K^{-1}	2.0
thermal capacity c	J kg^{-1} K^{-1}	840

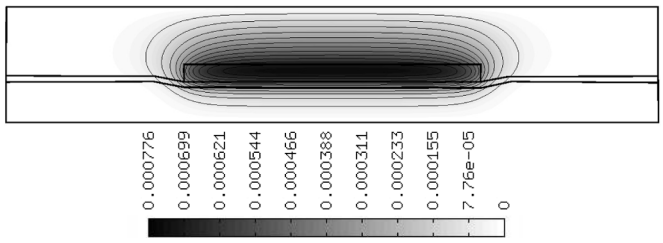

Fig. 2. Distribution of magnetic vector potential $|\underline{A}|_\alpha$ (Wb m^{-1}) in the system.

The automatic adaptation of hp-meshes significantly differs from the adaptivity in standard methods of this kind. This implies that traditional error estimates (one number per element) do not provide enough information to guide hp-adaptivity. One needs a better knowledge of the shape of the error function $e_{hp} = u - u_{hp}$, where u is the exact solution and u_{hp} the solution obtained in a particular step of the hp-process. In principle, it might be possible to obtain this information from estimates of higher derivatives, but this approach is not very practical. Usually it is easier to use a reference solution, i.e., an approximation $u_{\rm ref}$, which is at least by one order more accurate than u_{hp}. The hp-adaptivity is then guided by an a posteriori error estimate of the form $e_{hp} = u_{\rm ref} - u_{hp}$. More details on automatic hp-adaptivity on meshes with arbitrary level hanging nodes can be found in [6].

At each time level, optimal meshes are obtained automatically by independent adaptive processes. They dynamically change in time as the solution changes, respecting different features of particular fields (boundary layers, vortices, etc). This is possible as a result of our own multi-mesh technique that allows us solving multiphysics problems monolithically, even though each physical field is discretized on a geometrically different mesh. Thus, our approach leads to a significant reduction of the size of the discrete problem and speeds up the whole computation [7], [8]. In practical computations all physical fields are solved simultaneously, since the problem is coupled. But since the magnetic field changes in time very slowly, the solution from the previous level is used for the linearization of nonlinear terms in our equations. In the future,

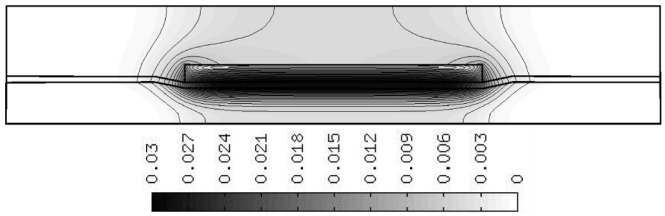

Fig. 3. Distribution of the module of magnetic flux density $|\boldsymbol{B}|$ (T) in the system (practically independent of time t).

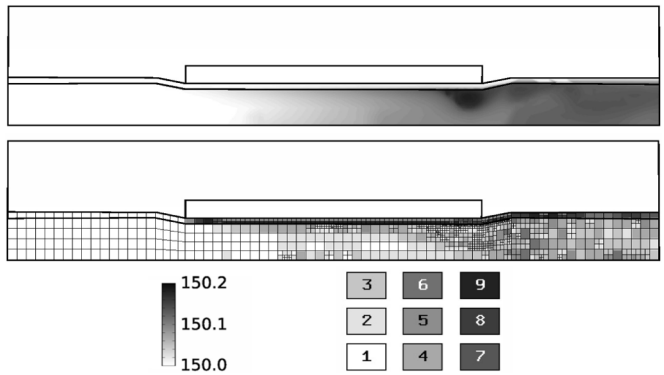

Fig. 4. Distribution of temperature T (°C) in the system after 10 s (up), adaptive mesh used for its computation at the same time (down), the grey rectangles with numbers inside show the orders of the corresponding elements.

we intend to apply nonlinear solvers to resolve nonlinearities contained in the problem more accurately.

Our own numerical software Hermes2D [3] was used for the computation. It is capable of all the features mentioned above, such as the higher-order finite element method, automatic adaptivity on hp-meshes or assembling the stiffness matrix on geometrically different meshes.

V. ILLUSTRATIVE EXAMPLE

A. Input Data

The pipe in Fig. 1 carries molten sodium whose inlet temperature $T_{\rm i} = 150$°C. At the time $t = 0$ (when the transport is considered steady-state) the inductor is switched on in order to warm up the melt. The distributions of the velocity and pressure in melt and temperature in the whole system melt-pipe for time $t = 0$ are known (they follow from the solution of the steady-state process before the inductor was switched on). The average value of velocity of melt at the inlet $v_{\rm ai} = 0.2$ ms^{-2}.

The parameters of the field current are $J_{\rm ext} = 10^6$ Am^{-2}, $f = 50$ Hz. The physical parameters of the molten sodium and basalt are given in Tables I and II.

B. Results and Discussion

First, we checked the convergence of the results related to the distribution of magnetic field with respect to the position of its artificial boundary. It was proved that particularly the position of its external part (see Fig. 2) does not need to be too far from the inductor. Although the magnetic field near this part of the boundary is strongly distorted, its values in melt do not change any longer.

Magnetic field and temperature are approximated on hp-meshes automatically obtained by our adaptive algorithm. An average size of hp-meshes for magnetic potential is around

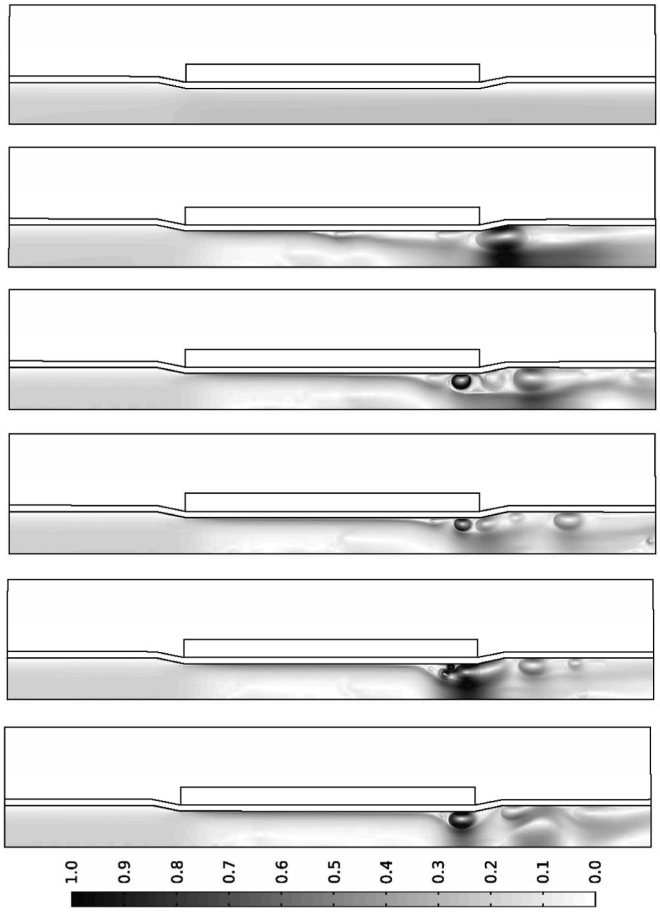

Fig. 5. Maps of the module of velocity $\boldsymbol{v}$ (ms^{-1}) in the pipe for $t = 0, 2, 4, 6, 8,$ and 10s (from the top to the bottom).

2700 degrees of freedom (DOFs), while h-adaptivity on biquadratic elements would result into mesh with around 17000 DOFs and reaching the same level of accuracy with uniform mesh and biquadratic elements requires more than 10^5 DOFs. Similar, however not that severe difference can be observed on hp-meshes for temperature field justifying need for higher-order FEM. For approximation of the flow field standard h-FEM adaptivity is used. The dynamically changing meshes for flow field are traveling together with moving vortices, resolving the flow features more accurately than we would obtain using a fixed uniform mesh.

Fig. 2 shows the distribution of magnetic field in the system. For low velocities of melt its values are practically the same as if we would omit in (1) the velocity term (the differences do not exceed about 2%).

Distribution of magnetic flux density $|B|$ in the domain is depicted in Fig. 3. This distribution practically does not depend on the velocity term in (1). The differences are the same as in the case of magnetic vector potential.

The temperature field does not change too much with time. Its distribution starts from the steady state before switching on the inductor. At time $t = 0$ this distribution is practically uniform both in melt and pipe and its value lies at maximum several hundredths of a degree below 150°C. Fig. 4 shows that even 10 s after switching on the inductor its distribution does not change by more than about 0.2°C.

Fig. 5 shows the time evolution of the flow field. Its maps for $t = 0, 2, 4, 6, 8,$ and 10 s are depicted from its top to the bottom. Visible is gradual generation of vortices at the right end of the thin part of the pipe.

VI. Conclusion

The described fully adaptive hp-FEM represents a powerful and efficient tool for numerical modeling of complicated coupled problems like that above. Its quality is really good and the speed of computations is very high.

Further research in the domain will be aimed at the acceleration of the existing algorithm, application of robust nonlinear solvers, parallelization of the code etc.

Acknowledgment

This work was supported by Research Plan MSM6840770017 and Grant Projects GA CR 102/07/0496 and GAASCR IAA100760702, both of which are gratefully acknowledged.

References

[1] P. A. Davidson, *An Introduction to Magnetohydrodynamics*. Cambridge: Cambridge Univ. Press, 2001.
[2] A. Alemany, P. Marty, and J. P. Thibault, *Transfer Phenomena in Magnetohydrodynamic and Electroconducting Flow*. Norwell: Kluwer, 1999.
[3] [Online]. Available: http://hpfem.org
[4] P. Solin, K. Segeth, and I. Dolezel, *Higher-Order Finite Element Methods*. Boca Raton: Chapman & Hall/CRC Press, 2003.
[5] G. Lube, "Stabilized Galerkin finite element methods for convection dominated and incompressible flow problems," *Num. Anal. Math. Model.*, vol. 29, pp. 85–104, 1994.
[6] P. Solin, J. Cerveny, and I. Dolezel, "Arbitrary-level hanging nodes and automatic adaptivity in the hp-FEM," *Math. Comput. Simul.*, vol. 77, pp. 117–132, 2008.
[7] P. Solin, J. Cerveny, L. Dubcova, and D. Andrs, "Monolithic discretization of linear thermoelasticity problems via adaptive multimesh hp-FEM," *J. Comput. Appl. Math.*.
[8] P. Solin, L. Dubcova, and J. Kruis, "Adaptive hp-FEM with dynamical meshes for transient heat and moisture transfer problems," *J. Comput. Appl. Math.*.